Papa, F., Güntner, A., Frappart, F., Prigent, C., Rossow, W. B. (2008): Variations of surface water extent and water storage in large river basins: A comparison of different global data sources. - Geophysical Research Letters, 35, L11401

DOI: 10.1029/2008GL033857

Variations of surface water extent and water storage in large river basins: A comparison of different global data sources.

F. Papa[(1)], A. Güntner[(2)], F. Frappart[(3)], C. Prigent[(4)], W. B. Rossow[(1)]

(1) NOAA-CREST, City College of New York, New York, USA; Email: papa@ee.ccny.cuny.edu
(2) GeoForschungsZentrum (GFZ), Potsdam, Germany
(3) CESBIO, Toulouse, France
(4) CNRS-LERMA, Observatoire de Paris, France

Abstract- For the period 2003-2004 and for six large river basins, the present study compares monthly time series of multi-satellite-derived surface water extent with other independent global data sets related to land water dynamics, such as water mass variations monitored by GRACE, simulated surface and total water storage from WGHM, water levels from altimetry, and GPCP precipitation estimates. In general, the datasets show a strong agreement with each other at seasonal timescale. In particular, over the Amazon and the Ganges basins, analysis of seasonal phase differences and hysteresis behaviour between surface water extent, storage and water level reveal the complex relations between water extent and storage variations and the different effects of water transport processes within large river basins. The results highlight the value of combining multi-satellite techniques for retrieving surface water storage dynamics.

1. Introduction.

Terrestrial water is critical to sustaining life on Earth and plays a primary role in the global water cycle and climate. Among the different reservoirs in which terrestrial water is stored, surface waters comprised of rivers, lakes, man-made reservoirs, wetlands, and episodically inundated areas are of particular importance because they interact more directly with the ocean and atmosphere through vertical and horizontal mass fluxes. In particular, analysis of variations in surface fresh water extent and storage is a key to understanding the hydrological processes and the global water cycle.

However, with approximately 60% of the world river floodplains and wetlands inundated only during some portion of the year [*Matthews*, 2000], seasonal and interannual variations in continental surface-stored water volumes at regional-to-global scales, as well as their impact on precipitation, evaporation, infiltration, and runoff, are still not well-known [*Bullock and Acreman*, 2003]. Lacking spatially complete measurements of inundation/wetland locations, sizes, and water volume changes, it is difficult to verify how hydrologic models properly partition precipitation among these several components and represent their effects on river discharge at continental-to-global scales [*Coe et al.*, 2002; *Alsdorf et al*., 2007a]. Consequently, the need for better long-term observations of land water extent and storage variations over the whole globe is now recognized [*Alsdorf et al.*, 2007a].

Remote sensing techniques have been very useful to hydrology investigations over the last fifteen years [*Alsdorf et al*., 2007a; *Alsdorf and Lettenmaier*, 2003]. For example, satellite altimetry has been used for systematic monitoring of water levels of large rivers, lakes, and floodplains [*Birkett*, 1998]. Interferometric synthetic aperture radars (SARs) have long been shown capabilities to study flood dynamics and their complexity, especially in the Amazon basin [*Alsdorf and Lettenmaier*, 2003; *Alsdorf et al.*, 2007b]. Since 2002, the GRACE gravity mission

47 offers, for the first time, direct estimates of the spatio-temporal variations of total terrestrial water
48 storage (the sum of ground water, soil water, surface water, and snow pack) [*Ramillien et al*.,
49 2005; *Schmidt et al.*, 2006] from month to several year timescales. However at this time, direct
50 estimates of surface water volume and their dynamics at continental/global scales are not
51 available and rely mainly on simulations from hydrological models.

52 *Frappart et al*. [2007] proposed a new technique to derive spatio-temporal variations of
53 surface water volume over the Negro River basin, the tributary which carries the largest discharge
54 volume to the Amazon River. The method is based on the combination of multi-satellite-derived
55 surface water extent estimates (~25km sampling intervals) [*Prigent et al.*, 2007; *Papa et al.*,
56 2006] and water levels over rivers and floodplains from both Topex/Poseidon (T/P) altimeter and
57 *in situ* hydrographic stations. Monthly surface water volume changes were produced with a
58 maximum error of 23 % over eight successive years (1993-2000), the period of common
59 availability of T/P and the multi-satellite data at this time. The estimates show excellent
60 agreement in the seasonal cycle with GRACE-derived total water mass variations.

61 The global dataset that quantifies the monthly distribution of surface water extent has been
62 extended to a 12-year record (1993-2004) [*Papa et al*., 2008] and now overlaps the GRACE
63 measurements for two entire years 2003-2004. The objective of the present study is to compare
64 the surface water extent dataset with other different and independent related land water
65 components and their variations at the scale of large river basins (Amazon, Ganges, Congo,
66 Mekong, Mississippi, Niger). These variables include surface and total water storage derived from
67 satellite (GRACE) and modelling (WGHM), precipitation estimates (GPCP), T/P altimeter-
68 derived inland water-body level heights and *in situ* river discharge. These comparisons will help
69 better illustrate the complex relations between surface water extent and storage at the scale of
70 large river basins and highlight the value of using multi-method and multi-satellite techniques to

71 retrieve surface water storage dynamics and improve our understanding of the terrestrial water
72 cycle.
73
74 **2. Data sets.**
75 In this study, the analysis includes:
76 1) A dataset that quantifies at global scale the monthly distribution of surface water extent
77 (SWE) and its variations at ~25km sampling intervals. The methodology which captures the
78 extent (with an accuracy of ~10%) of episodic and seasonal inundations, wetlands, rivers, lakes,
79 and irrigated agriculture over more than a decade, 1993-2004, is based on a clustering analysis of
80 a suite of complementary satellites observations, including passive (SSM/I) and active (ERS)
81 microwaves, visible and near-IR (AVHRR) observations [*Prigent et al*., 2007; *Papa et al*., 2006,
82 2008].
83 2) the GRACE-derived land water mass solution. The GRACE mission, launched on the 17th
84 of March 2002, is devoted to measuring spatio-temporal changes in Earth's gravity field . Several
85 recent studies have shown that GRACE data over the continents provide important information on
86 the total land water storage [*Schmidt et al., 2006;*; *Ramillien et al*., 2005] with an accuracy of
87 ~1.5 cm of water thickness equivalent when averaged over a few hundred kilometers. Here we use
88 the three latest land water solutions (RL04) provided by GFZ, JPL (for these two first products,
89 January 2003, June 2003 and January 2004 are missing), and CSR (June 2003 and January 2004
90 are missing) with a spatial resolution of ~400km and processed as in *Chambers* [2006]. These
91 three datasets are available at http://gracetellus.jpl.nasa.gov/.
92 3) Surface and total water storage from the WaterGAP Global Hydrology Model (WGHM).
93 WGHM represents the continental water cycle at 0.5° spatial intervals [*Döll et al*., 2003],
94 including its most relevant water storage components (snow, soil water, groundwater, surface

95 water in rivers, lakes, and wetlands). WGHM has been widely used to analyze spatio-temporal
96 variations of water storage components globally and for large river basins [*Güntner et al*., 2007].
97 In this study, we use the latest WGHM version as described in Hunger and Döll [2007], extending
98 the simulation period until 2007 by using climate forcing data in terms of monthly precipitation
99 from the Global Precipitation Climatology Centre (GPCC) [*Rudolf and Schneider*, 2005] and air
100 temperature, radiation, and number of raindays within each month from the European Centre for
101 Medium-Range Weather Forecast (ECWMF) operational forecasts.

102 4) Precipitation estimates from the Global Precipitation Climatology Project (GPCP) that
103 quantify the distribution of precipitation over the global land surface [*Adler et al*., 2003]. We use
104 the Satellite-Gauge Combined Precipitation Data product Version 2 data, whose estimates
105 uncertainties over land range between 10%–30%. Note that the GPCC data used to force WGHM
106 are the *in situ* component of GPCP.5) Topex/Poseidon (T/P) radar altimeter-derived water level
107 heights over large water bodies. First devoted to ocean studies, T/P is commonly used to monitor
108 water levels over lakes, rivers and floodplains [*Birkett*, 1998] and provide time series of
109 river/inundation level variations from 1993 to mid-2002, before its orbit was changed. In this
110 study, we use the data from the HydroWeb database ([*Gennero et al*., 2005] available at
111 http://www.legos.obs-mip.fr/en/soa/hydrologie/hydroweb/). For the selected points here, the
112 uncertainty associated with the water level height over the Amazon and the Ganges basins ranges
113 between 10-30 cm for high water season to 30-80 cm during low water season.

114 **3. Results and discussion.**

115 Figure 1 compares the monthly time series of precipitation, SWE and the surface and total
116 water storage over 2003-2004 for six large river basins (the data are aggregated to basin
117 averages), representing different environments from tropical, mid-latitudes, and semi-arid
118 regions. For each time series, the 2-year mean is removed and the resulting anomalies are

normalized by their standard deviations. Table 1 summarizes the maximum linear correlation coefficients of point time records between the SWE and the other variables when lagged in time (months). In view of the short time span considered here, the signal is dominated by seasonal variations. Regardless of the environment, Figure 1 and Table 1 show that the seasonal patterns of the time series are similar and show highly significant correlations.

For the Amazon basin, the time records in Figure 1a and Table 1 show that the annual variations of precipitation lead the variations of the surface water extent by 2 months (R=0.84 with a lag of 2 months). This time lag illustrates that, first, a considerable amount of inundation-bearing runoff is generated only after refilling of soil and groundwater storages with some delay in the rainy season, and that, secondly, stream flow from upstream regions contributes with a delay in time to large downstream flooding due to the long concentration times in the large hydrographic network of the Amazon. The seasonal variation of SWE is in phase with the surface and total water storage variations (R>0.89). This implies that inundation area may be a good indicator of actual surface water volumes in this basin and supports earlier studies showing that mass variations in surface water bodies in the Amazon basin contribute significantly to the total storage variations [*Matsuyama and Masuda*, 1997; *Güntner et al.*, 2007]. Too large large-scale water transport velocities in the model may explain that the simulated surface water storage leads the annual cycle of the other variables by 1 month.

For the Ganges basin (Figure 1b), which receives intense local rainfall during the annual monsoon, the precipitation and the SWE are highly correlated with no lag in time (R=0.93). SWE variations lead variations in volume storage from GRACE and WGHM by one month with R>0.79. As for the Ganges, SWE of the Mekong (Figure 1d) and the Niger (figure 1f) basins are also controlled by large precipitation events during the rainy season with a delay of 1 month relative to the rainfall variations. For both basins, the storage variables follow closely the

143 seasonality of SWE also with a delay of 1 month (R>0.89), except for the simulated surface
144 water storage.

145 The Congo and the Mississippi basins, Figure 1c and e, exhibit less agreement between the
146 different variables, especially regarding the amplitude of the signal. The Congo SWE shows a fair
147 correlation with the precipitation and GRACE variations but a poor agreement with the simulated
148 surface water storage from WGHM. The disagreement of total water storage between WGHM
149 and GRACE over the Congo reveals the difficulty of hydrological models to properly represent
150 the complexity of the entire Congo basin. Congo sub-basins have different responses to rainfall in
151 terms of flood and storage dynamics due to different soil properties across the basin [*Laraque et*
152 *al*., 2001]. In addition, during periods of high anomaly in precipitation (for instance early 2003
153 and end 2004), 60-70% of rainfall is lost by runoff and evapotranspiration [*Crowley et al*., 2006].
154 For the Mississippi, the SWE estimates show a lower correlation with GRACE and poor
155 agreement with the precipitation estimates and the simulated volume storage. These generally
156 lower correlations show that surface water storage is a minor contribution to total storage in the
157 Mississippi watershed [*Lettenmaier and Famiglietti*, 2006] and that the basin hydrology is
158 complicated by the flood dynamics partially driven by spring snowmelt in the upper portions of
159 the basin.

160 Phase differences between precipitation, water surface extent, and water storage observed in
161 Figure 1 and in the lagged temporal correlations in Table 1 reveal the different effect of water
162 transport processes within large river basins. A delay of the seasonal cycle of water extent
163 relative to precipitation (Amazon, Mekong, Niger) indicates the large water travel and
164 accumulation times in large river basins that may lead to inundation at downstream locations of
165 the basin even if the basin-average rainfall maximum has been passed. Focusing on the Amazon
166 and the Ganges basins, Figure 2 illustrates two different cases of the complex dynamics between

167 the variations in the SWE and the variations in the surface and total water storage. Figure 2
168 compares the mean seasonal cycle 2003-2004 (for available months) between the SWE and the
169 total water storage from GRACE CSR (Figure 2a and 2d) and between the SWE and the
170 simulated surface water storage from WGHM (Figure 2b and 2e). We also compare here the
171 normalized mean seasonal cycle calculated over 1993-2000 between the SWE and the altimeter
172 level height from T/P for some locations across the two basins (Figure 2c for the Amazon and 2f
173 for the Ganges). In *Frappart et al.* [2007], we demonstrated that surface water volume change
174 can be derived from the multi-satellite SWE combined with T/P water level heights. Over the
175 Amazon, we also display the mean seasonal cycle 1993-2000 for the *in situ* river discharge at
176 Obidos (2.50S; 55.51W) a location close to the altimeter level measurements (at 2.50S; 56.50W).
177 Figure 2 clearly shows that the two basins exhibit different regimes with different
178 hydrological phases. For the Amazon, Figures 2a and 2b show that the mean annual cycle can be
179 divided into sub-periods where the SWE and the volume storage varying together: a low water
180 period from September to November, a rising period from January to April, a high water period
181 in April-May and a falling period from June to September. The surface storage and the total
182 storage show differences with a quicker decrease of surface storage during the period of
183 decreasing inundation area. This suggests a longer residence time of soil water and groundwater
184 as part of total storage, but may also point to model deficiencies, i.e., too rapid surface water
185 transport. In addition, Figure 2c clearly shows that the mean annual cycles between the SWE, the
186 water level height, and the discharge have patterns close to the ones observed between the SWE
187 and the volume storages. In the case of the Amazon, SWE and water stage increase/decrease
188 roughly simultaneously, leading to an approximately unique relationship between water
189 extent/level and volume for aggregated basin-scale values.

190 The Ganges basin shows a totally different regime than the Amazon basin, with a strong
191 hysteresis behaviour between the SWE and the storage components (Figure 2d and 2e). The
192 minimum period is from January to May and the rising period shows a large increase of both
193 SWE and water storage as the monsoon season starts. With the SWE at maximum in July, surface
194 and total water volume are still increasing in August. The falling period, from September to
195 December, shows a sharp decrease in SWE while water storage remains high and decreases more
196 slowly. Figure 2f shows a similar behaviour between the SWE and the water level heights and
197 confirms a strong hysteresis pattern, especially for downstream locations in the river basin (black
198 and red). In these cases, due to large water transport times through the river network, high water
199 levels occur comparatively late in the monsoon season when inundation in the upstream parts of
200 the basin are at the maximum or starting to decline. The hysteresis between water extent and
201 storage indicates widespread shallow flooding in the river basin with the onset of the monsoon
202 period, including flooding of irrigated agricultural areas (e.g. paddy fields). These shallow
203 inundation areas rapidly dry out after the end of the rainy season (see the high correlation without
204 time lag between precipitation and water extent in Table 1), while large water masses remain
205 stored in the main floodplains and the delta regions which continue to receive water from the
206 entire watershed and additional precipitation.
207
208 **5. Conclusion.**
209 This study reports a first effort to compare and analyze the variations of multi-satellite-
210 derived surface water extent with precipitation estimates, water mass variations monitored by
211 GRACE and surface and total water storage simulated by WGHM. Over six major river basins
212 and for a 2-year period (2003-2004), the different data sets show in general good agreement in
213 their seasonal variations. Over the Amazon and the Ganges, analyses of phase differences and

hysteresis behaviour in the mean annual cycle between surface water extent, water level height, and water storage demonstrate the complex relationships between these variables at the scale of large river basins. Figure 2 In particular, the delay with which an increase in inundation extent translates into a major increase of surface water volumes depends on the water transport processes and flow concentration times of a certain river basin. The results highlight that a combination of the surface water extent dataset and altimeter-derived water level height in order to derive surface water volume change, as proposed in *Frappart et al*., [2007] over the Negro Rio, could be successfully applied to other large river basins. In combination with near-future soil moisture products derived from SMOS, it will allow for the first time a decomposition of the total water storage monitored by GRACE into its several components.

References

Adler, R. F., G. J. Huffman, A. Chang, R. Ferraro, P. Xie, J. Janowiak, B. Rudolf, U. Schneider, S. Curtis, D. Bolvin, A. Gruber, J. Susskind, and P. Arkin (2003), The Version 2 Global Precipitation Climatology Project (GPCP) Monthly Precipitation Analysis 1979-Present, *J. Hydrometeor.*, *4*, 1147-1167.

Alsdorf, D. E., and D. P. Lettenmaier (2003), Tracking fresh water from space, *Science*, 301, 1492-1494.

Alsdorf, D. E., E. Rodríguez, and D. P. Lettenmaier (2007a), Measuring surface water from space, *Rev. Geophys*., 45, RG2002, doi:10.1029/2006RG000197.

Alsdorf, D., P. Bates, J. Melack, M. Wilson, and T. Dunne (2007b), Spatial and temporal complexity of the Amazon flood measured from space, *Geophys. Res. Lett*., 34, L08402, doi:10.1029/2007GL029447.

Birkett, C. M. (1998), Contribution of the TOPEX NASA radar altimeter to the global monitoring of large rivers and wetlands, *Water Resour. Res*., 34 (5), 1223-1239.

238 Bullock, A., M.C. Acreman (2003), The role of wetlands in the hydrological cycle, *Hydrol. Earth*
239 *Syst. Sci., 7(3)*, 75-86.
240 Chambers, D.P.: Evaluation of New GRACE Time-Variable Gravity Data over the Ocean.
241 *Geophys. Res. Lett.*, 33(17), LI7603, 2006.
242 Coe, M. T., M. H. Costa, A. Botta, and C. Birkett (2002). Long-term simulations of discharge and
243 floods in the Amazon Basin, *J. Geophys. Res.*, 107(D20), 8044,
244 doi:10.1029/2001JD000740.
245 Crowley, J. W., J. X. Mitrovica, R. C. Bailey, M. E. Tamisiea, and J. L. Davis (2006), Land water
246 storage within the Congo Basin inferred from GRACE satellite gravity data, *Geophys.*
247 *Res. Lett.*, 33, L19402, doi:10.1029/2006GL027070.
248 Döll, P., F. Kaspar, and B. Lehner (2003), A global hydrological model for deriving water
249 availability indicators: model tuning and validation, *J. Hydro,* (270)- 105-134.
250 Frappart F., F. Papa, J. S. Famiglietti, C. Prigent, W. B. Rossow, and F. Seyler (2007),
251 Interannual Variations of River Water Storage from a Multiple Satellite Approach: A case
252 study for the Rio Negro River basin, *J. Geophys. Res*, under revison.
253 Gennero, M. C., J. F. Cretaux, M. Berge NGuyen, C. Maheu, K. Do Minh, S. Calmant, and A.
254 Cazenave (2005), HydroWeb, Surface water monitoring by satellite altimetry, Laboratoire
255 d'Etudes en Géodésie et Oceanographie Spatiale, Toulouse, France.
256 Güntner, A., J. Stuck, S. Werth, P. Döll, K. Verzano, and B. Merz (2007), A global analysis of
257 temporal and spatial variations in continental water storage. *Water Resour. Res.*, 43(5):
258 W05416, DOI 10.1029/2006WR005247.
259 Hunger, M., and P. Döll (2007), Value of river discharge data for global-sale hydrological
260 modeling, *Hydrology and Earth System Sciences Discussion*. 4, 4125-4173.

261 Laraque, A., G. Mahe, D. Orange, and B. Marieu (2001), Spatiotemporal variations in
262 hydrological regimes within Central Africa during the XXth century, *J. Hydro.*, 25,
263 doi:10.1016/S0022-1694(01)00340-7.
264 Lettenmaier, D. P., and J. S. Famiglietti (2006), Hydrology - Water from on high, *Nature*, 444,
265 562-563.
266 Matsuyama, H., and K. Masuda (1997), Estimates of continental-scale soil wetness and
267 comparison with the soil moisture data of Mintz and Serafini. *Climate Dynamics*,
268 13(10):681-689.
269 Matthews, E. (2000*), Wetlands in Atmospheric methane: its role in the global environment*,
270 edited by M. A. K. Khalil, pp. 202-233, Springer-Verlag, New York.
271 Papa, F., C. Prigent, F. Durand, and W. B. Rossow (2006), Wetland dynamics using a suite of
272 satellite observations: A case study of application and evaluation for the Indian
273 Subcontinent. *Geophys. Res. Lett., 33*, L08401, doi:10.1029/2006GL025767.
274 Papa F., Prigent, C., W. B. Rossow, and E. Matthews (2008), Inter-annual variability of surface
275 water extent at global scale, 1993-2004, *J. Geophys. Res*, under review.
276 Prigent, C., F. Papa, F. Aires, W. B. Rossow, and E. Matthews (2007), Global inundation
277 dynamics inferred from multiple satellite observations, 1993-2000, *J. Geophys. Res*., 112,
278 D12107, doi:10.1029/2006JD007847.
279 Ramillien G., F. Frappart, A. Cazenave, and A. Güntner (2005), Time variations of the land water
280 storage from an inversion of 2 years of GRACE geoids, *Earth Planet. Sci. Lett*., 235,
281 283-301.
282 Rudolf, B. and U. Schneider (2005), Calculation of Gridded Precipitation Data for the Global
283 Land-Surface using in-situ Gauge Observations, Proceedings of the 2nd Workshop of

the International Precipitation Working Group IPWG, Monterey, October 2004, 231-247.

Schmidt, R., P. Schwintzer, F. Flechtner, C. Reigber, A. Güntner, P. Döll, G. Ramillien, A. Cazenave, S. Petrovic, H. Jochmann, and J. Wünsch (2006), GRACE observations of changes in continental water storage, *Global and Planetary Change*, 50, 112-126.

Table 1: Maximum time-lagged linear correlation coefficient (with the time-lagged in month in brackets) between the surface water extent and the precipitation, the total water storage from GRACE and the simulated water storage from WGHM for the 6 basins. For instance over the Amazon, the surface water extent and the precipitation have a maximum correlation of 0.84 with the precipitation preceding the surface water extent with 2 months. For the comparison with the precipitation and the model (24 months), p-values<0.01 for R>0.51 , with GRACE-CSR (22 months), p-values<0.01 for R>0.53 and with GRACE-JPL and GFZ (21 months), p-values<0.01 for R>0.55.

		Precipitation (mm/month)	Total Water Storage (km^3)			Water storage (km^3) WGHM	
		GPCP	GFZ	JPL	CSR	Surface	Total
Surface water extent (km^2)	Amazon	0.84 (-2)	0.95	0.95	0.95	0.93 (-1)	0.89
	Ganges	0.93	0.79 (+1)	0.79 (+1)	0.79 (+1)	0.84 (+1)	0.84 (+1)
	Congo	0.71	0.83	0.83	0.85	0.69 (+1)	0.61
	Mekong	0.89 (-1)	0.89 (+1)	0.89 (+1)	0.89 (+1)	0.94	0.94 (+1)
	Mississippi	0.48 (+1)	0.69	0.69	0.69	0.51	0.61 (-2)
	Niger	0.90 (-1)	0.86 (+1)	0.86 (+1)	0.84 (+1)	0.81 (+1)	0.94

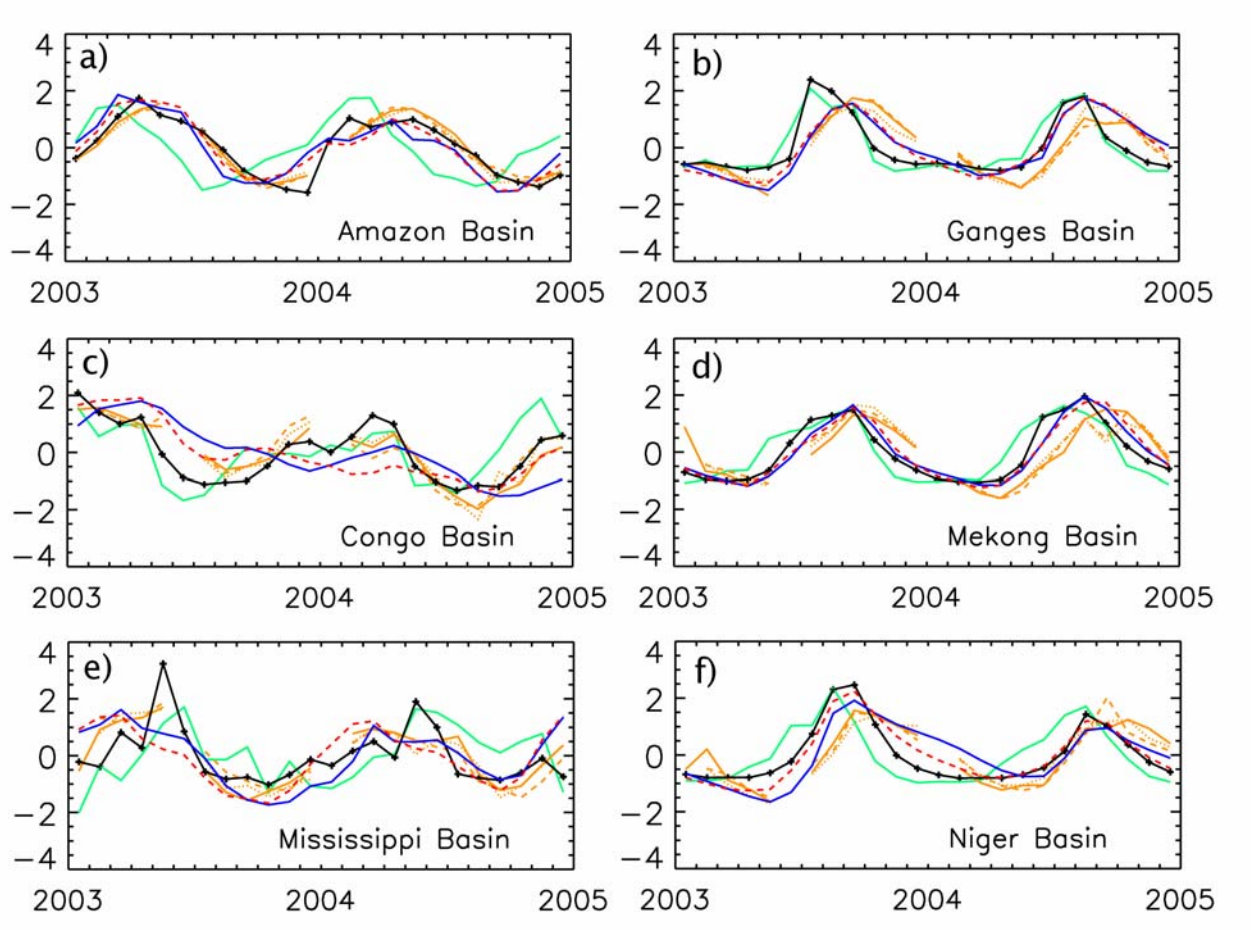

Figure 1: Time series of satellite-derived inundation extent (black), GRACE-derived total water storage (yellow; version 4 from CSR solid line; version 4 from GFZ dotted line, version 4 from JPL dashed line), WGHM simulated total water storage (dashed red), WGHM simulated surface water storage (blue) and GPCP precipitation (green) for six large river basins during the 2003 – 2004 period. All variables are normalized (the mean is subtracted and the resulting values are divided by the standard deviation over the period).

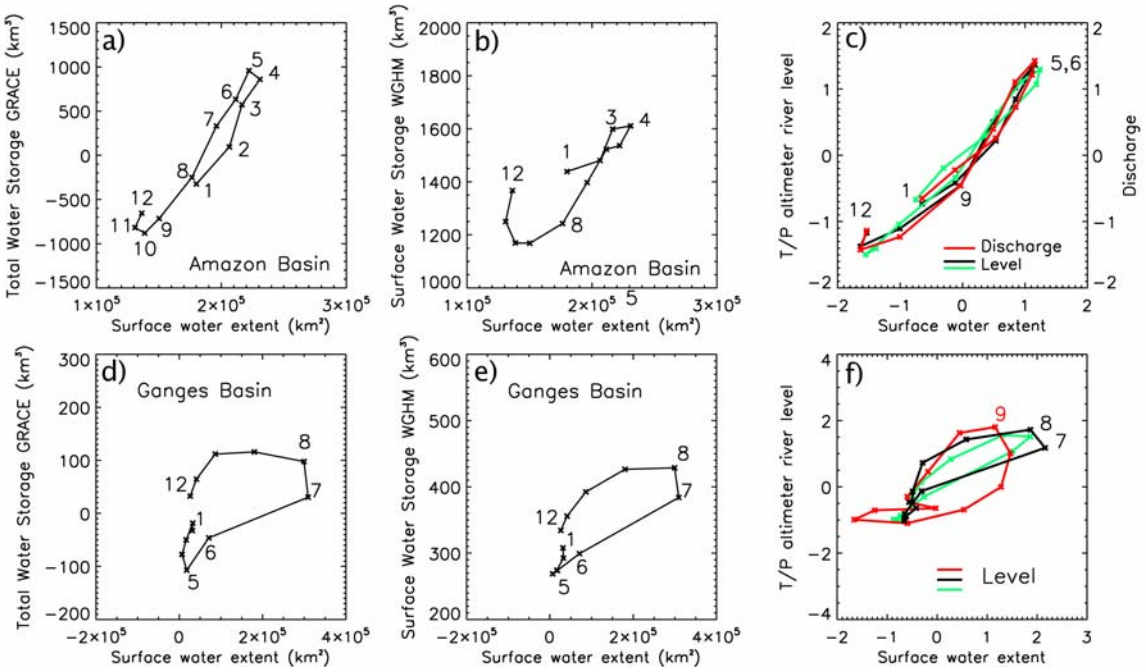

Figure 2:

a), d) Mean seasonal cycle between the satellite-derived surface water extent and GRACE-derived total water storage version 4 from CSR for the Amazon and the Ganges basins during the 2003 – 2004 period (the numbers represent the month of the year);

b), e) 2003 – 2004 mean seasonal cycle between the multi-satellite-derived surface water extent and WGHM simulated surface water storage;

c) mean seasonal cycle (normalized anomaly) between the satellite-derived surface water extent and altimeter-derived river level heights (black for (2.50S;56.50W), green for (-3.23S;59.50W)) and between the *in situ* river discharge at Obidos (red (2.50S;55.51W)) for the Amazon;

f) mean seasonal cycle (normalized anomaly) between the satellite-derived surface water extent and altimeter-derived river level height for the Ganges (black for (27.93N;78.86E), green for (25.50N;85.70E), red for (23.27N;89.55E));

For c) and f), the mean cycles are calculated over the period 1993-2000 and the surface water extent is calculated on a 2^{o}x2^{o} area centered on the altimeter water level estimates.